Hindawi
Mathematical Problems in Engineering
Volume 2018, Article ID 7614304, 12 pages
https://doi.org/10.1155/2018/7614304

Research Article

Electric Power Steering System Control Strategy Based on Robust H∞ Control for Electric Forklift

Zhizheng Jiang[1,2] **and Benxian Xiao**[1,2]

[1]*School of Electrical Engineering and Automation, Hefei University of Technology, Hefei 230009, China*
[2]*Institute of Industry & Equipment Technology, Hefei University of Technology, Hefei 230009, China*

Correspondence should be addressed to Benxian Xiao; xiaobenxian@126.com

Received 23 April 2018; Revised 28 July 2018; Accepted 26 August 2018; Published 9 September 2018

Academic Editor: Jorge Rivera

The dynamic model of the Electric Power Steering (EPS) system for electric forklifts and the two-degree-of-freedom (2DOF) forklift models has been established. Based on the control target of electric forklift EPS, a generalized EPS control model with model perturbation and interference is established. The standard H∞control model of the EPS system is transformed, and the EPS generalized state equation of electric forklift is derived. The principle of robust control with genetic optimization is expounded, aiming at the parameters optimization of the weighted function of H∞control model, the constraint function of the genetic algorithm (GA) is constructed, and the robust controller of genetic optimization is derived. Taking the electric forklift TFC20 as the research object, according to the actual data on the forklift, the system model is established in MATLAB, and the effects of PID control, robust control, and genetic robust control are compared, the results show that the power steering characteristic of the robust control is better than the power steering characteristic of the PID control, and the stability of the forklift under the control of robust control is better. Also, the power steering characteristic of the H∞ controller with GA optimization is better than that of an unoptimized one, and its robustness is better, under external pavement interference, the following ability is stronger for the ideal current and the steering is more stable.

1. Introduction

EPS system is a kind of power steering system is which widely used in the field of vehicles; the system helps the driver to complete the steering movement by providing appropriate power and controlling the motor through the electronic control unit, in order to improve the steering performance of the vehicle. In recent years, many researchers have conducted in-depth research on vehicle's electric power steering system model, vehicle's power characteristics curve, and vehicle's control strategy, and some intelligent algorithms have been used in vehicle's electric power steering system.

"Fan L et al." [1] proposed that considering the EPS control strategy of tire-road friction, the steering system model, nonlinear vehicle dynamics model, and tire model are developed under MATLAB/Simulink. Simulation results show that the new EPS-assisted control strategy can improve the steering efficiency under sliding condition. "Hung Y C et al" [2] pointed that the wavelet fuzzy neural network with asymmetric membership function and the improved differential evolution algorithm are used to control the EPS system of six-phase PMSM to improve the driver's comfort and the stability of the vehicle, and the experimental verification was given. "Wonhee Kim et al." [3] presented robust steering angle control of electric power steering of vehicle automatic lane keeping system based on moment superposition; this method includes an enhanced observer and a nonlinear damping controller, and the effectiveness of the control method was verified by a test car. "Dongwook Lee et al." [4] designed a nonlinear torque diagram, which reflects the mapping relationship between driver torque and power motor torque and vehicle speed. In addition, the design criteria of a stabilizing compensator are also proposed. In the simulation, lead-to-lag compensator with different parameters is used. "Gong J Q et al" [5] proposed that based on particle swarm optimization of heavy truck EPS

system control strategy is proposed, on the basis of vehicle EPS system overall design, taking DC motor current as the control target, using particle swarm optimization fuzzy control strategy, using MATLAB/Simulink as simulation platform, and taking dump truck as research type models and commercial vehicle simulation model which equipped with EPS system is established. And their simulation experimental results show that, compared with the conventional fuzzy control, particle swarm optimization fuzzy control can improve the whole dynamic response of heavy truck EPS system efficiently, also good steering portability and handling stability is obtained. Other researchers used fuzzy control [6, 7], variable structure control [8], LQR control [9, 10], disturbance observer [11], sliding mode control [12, 13], robust and H∞ control [14–16], optimization algorithm [17, 18], friction compensation control [19], road feeling [20], and so on for vehicle steering system control. These research results are mostly for passenger cars. Forklift, as a kind of industrial handling vehicle, has its own unique operating properties and it is widely used to complete the cargo handling and loading operations in the factory workshop, storage logistics centers, and warehouse shelves. The weight of forklift is large, the working environment is small and complex, so the turning radius should be small, and if the steering is unstable which will leads to rollover and other serious accidents, these factors make the forklift steering characteristics and stability become a high degree of concern problem.

In order to improve the steering stability of electric forklift, this paper takes the TFC20 front steering electric forklift produced by Hefei Banyitong Science and Technology Development Co. Ltd., as the research object and aiming at the parameters optimization of the weighted function in H∞ control model, the constraint function of GA is constructed, and the robust controller with genetic optimization is designed and the stability of the controller is analyzed and verified by simulation.

2. Electric Forklift EPS Model and Control Target

2.1. Steering Mechanism Model. The TFC20 front-wheel steering electric forklift used in this paper has shaft-assisted EPS steering structure. This kind of EPS steering structure can provide electric power torque well with DC motor and it is also very suitable for medium-load electric forklift. Shown in Figure 1 is the shaft-assisted EPS steering structure.

During the forklift driving process, the EPS system is mainly affected by the moments of the operating torque, the moments of the power torque, and the moments of the steering resistance torque, and the balance of the three torques needs to be maintained. According to Newton's law and Kirchhoff's law, the force balance equation of each part of electric forklift EPS system is as follows [21–23]:

Hand-wheel:

$$J_s\ddot{\alpha} + B_s\dot{\alpha} = T_h - T_c + f_s(\alpha, \dot{\alpha}) \tag{1}$$

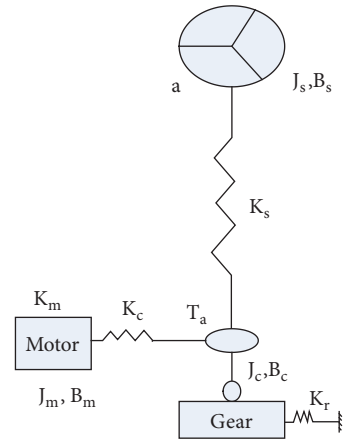

Figure 1: The shaft-assisted EPS steering structure.

Output shaft:

$$J_c\ddot{\delta} + B_c\dot{\delta} = T_\alpha + T_c - T_f + f_c(\delta, \dot{\delta}) \tag{2}$$

Motor:

$$\begin{aligned} J_m\ddot{\theta} + B_m\dot{\theta} &= T_m - \frac{T_\alpha}{g_1} + f_m(\theta, \dot{\theta}) \\ T_m &= K_t * i \\ u &= Ri + L\dot{i} + K_e\dot{\theta} \end{aligned} \tag{3}$$

On the condition of small steering corner, the characteristics of the tire are approximately linear. It can be derived that the torque $T_f{}'$ (around the steering pin) acting on the tire is

$$T_f{}' = K_\rho\delta' \tag{4}$$

where δ' is the front wheel angle, and the front wheel angle δ' and the output shaft angle δ have the following relationship:

$$\delta = \delta' * g_2 \tag{5}$$

The torque $T_f{}'$ (around the steering pin) acting on the tire and the tire torque T_{f_1} acting on the output shaft have the following relationship:

$$T_{f_1} = T_f{}' * g_2 \tag{6}$$

Neglecting the effect of air resistance on the electric forklift, simplifying the system, and then deriving the equivalent resistance torque to the output shaft are as follows:

$$T_f = K_c\delta + T_r \tag{7}$$

And

$$\begin{aligned} T_c &= K_s(\alpha - \delta) \\ T_\alpha &= K_m(\theta - \delta) \\ k &= \mathrm{f}(T_h \;\; G_1 \;\; u_1) \\ i_m &= kT_c \end{aligned} \tag{8}$$

As the inductance value "L" is small when the motor current is stable, the nonlinear part of the motor is ignored in the analysis and the following equation can be obtained:

$$T_m = \frac{K_t}{R}\left(\mathrm{u} - K_e\dot{\theta}\right) \tag{9}$$

Interpretation of variables is shown in Nomenclature.

2.2. State Equation of Steering Mechanism. To simplify the discussion of the problem, here we temporarily ignore the nonlinear part of the EPS-related component, i.e., ignoring the effect of $f_s(\alpha, \dot{\alpha})$, $f_c(\delta, \dot{\delta})$, $f_m(\theta, \dot{\theta})$, and represent the state equation as a linear part. These nonlinearities, together with the external disturbances to the system, cause uncertainty in the steering system of the electric forklift, which is expressed as the uncertainty of the system and will be explained in the next chapter. The standard state equation expression for the system is as follows:

$$\begin{aligned} \dot{x} &= Ax + BU \\ y &= Cx + DU \end{aligned} \tag{10}$$

where state vector is

$$x = \begin{bmatrix} x_1 & x_2 & x_3 & x_4 & x_5 & x_6 \end{bmatrix}^T = \begin{bmatrix} \alpha & \dot{\alpha} & \delta & \dot{\delta} & \theta & \dot{\theta} \end{bmatrix}^{\mathrm{T}}; \tag{11}$$

control signal U is

$$U = \begin{bmatrix} d & u \end{bmatrix}^{\mathrm{T}} = \begin{bmatrix} T_h & T_r & u \end{bmatrix}^{\mathrm{T}}; \tag{12}$$

system output y is

$$y = [i]; \tag{13}$$

Then the coefficients of the standard equation of state are as follows:

$$A = \begin{bmatrix} 0 & 1 & 0 & 0 & 0 & 0 \\ \frac{-K_s}{J_s} & \frac{-B_s}{J_s} & \frac{K_s}{J_s} & 0 & 0 & 0 \\ 0 & 0 & 0 & 1 & 0 & 0 \\ \frac{K_s}{J_c} & 0 & \frac{-\left(K_m + K_s + K_c\right)}{J_c} & \frac{-B_c}{J_c} & \frac{K_m}{J_c} & 0 \\ 0 & 0 & 0 & 0 & 0 & 1 \\ 0 & 0 & \frac{K_m}{g_1 * J_m} & 0 & \frac{-K_m}{g_1 * J_m} & \frac{-\left(\left(K_t * K_e\right)/(R+L) + B_m\right)}{J_m} \end{bmatrix}$$

$$B = \begin{bmatrix} 0 & \frac{1}{J_s} & 0 & 0 & 0 & 0 \\ 0 & 0 & 0 & \frac{1}{J_c} & 0 & 0 \\ 0 & 0 & 0 & 0 & 0 & \frac{K_t}{J_m * (\mathrm{R} + \mathrm{L})} \end{bmatrix}^{\mathrm{T}}$$

$$C = \begin{bmatrix} 0 & 0 & 0 & 0 & 0 & -\frac{K_e}{R} \end{bmatrix}$$

$$D = \begin{bmatrix} 0 & 0 & \frac{1}{R} \end{bmatrix} \tag{14}$$

2.3. The 2DOF Model of the Electric Forklift. In order to better analyze the steering stability of electric forklift, combined with the TFC20 front steering electric forklift, the 2DOF model of the forklift is established as follows [24, 25]:

$$\begin{aligned} \left(k_1 + k_2\right)\beta + \frac{1}{u_1}\left(ak_1 - bk_2\right)\omega_r - k_1\delta &= m\left(\dot{v} + u_1\omega_r\right) \\ \left(ak_1 - bk_2\right)\beta + \frac{1}{u_1}\left(a^2k_1 + b^2k_2\right)\omega_r - ak_1\delta &= I_z\dot{\omega}_r \end{aligned} \tag{15}$$

where k_1, k_2 are the lateral stiffness of front and rear tire, respectively. a is the distance from vehicle centroid to the front axle, b is the distance from vehicle centroid to the rear axle, m means the quality of the vehicle, ω_r means the yaw rate, β means the sideslip angle, v stands for the component of velocity along the Y axis, and I_z represents the forklift's moment of inertia about Z axis.

2.4. Control Target. The EPS system should be portability when it is turned in place or turned at low speed. Compared to the car, the steering of the electric forklift is more frequent and, in most cases, the turning radius of the steering operation is the minimum; therefore the driver's steering force should be reduced.

During the electric forklift driving process, the driver can get a good sense of the road, which makes the EPS

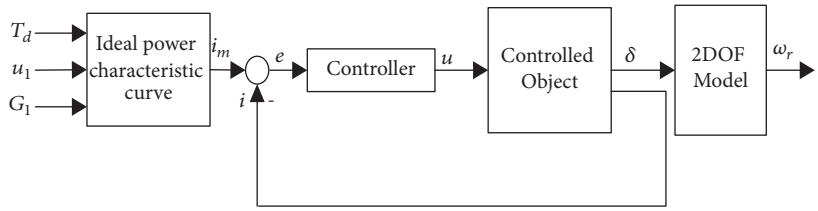

Figure 2: Structure of EPS control system.

system have a good flexibility and when the electric motor provides enough electric power torque to the electric forklift, the operation of the driver can be very portable, but this also leads to a lack of a sense of the road to the driver.

Therefore, the goal of this paper is to balance the "portability" and "flexibility" of the EPS system. At the same time, we should pay attention to the safety and stability of the steering.

Set the following two control targets.

(1) Error of the Power e

$$e = T_a - T_a^* \tag{16}$$

where $T\alpha$ is the actual power value provided by the motor and $T\alpha*$ is the ideal power value which the motor should provide.

(2) Yaw Rate ω_r. The yaw rate represents the stability of the operation of the electric forklift, so setting this goal we hope that, in the case of interference, the steering of electric forklift is still has good yaw rate response, the structure of EPS control system is shown in Figure 2.

The working principle of the system is as follows: firstly, the desired motor current is obtained from the ideal power characteristic curve; then let desired motor current minus the actual current obtain the current difference. Input the current difference to the controller and, according to the appropriate control algorithm, the appropriate motor control voltage will be output, and then the desired motor current will be obtained. At the same time, combining the input of the hand-wheel angle and 2DOF model, the response curve of the yaw rate of the forklift can be obtained, and then we can observe the steering stability of the electric forklift.

3. Robust Control Model

Robust control is to quantitatively investigate the model error of the system and investigate the ability of the system to maintain its performance under bounded interference. For linear systems, the nominal object transfer function G (s) and unknown perturbation Δ (s) are often used to characterize the uncertain system.

The problem of H∞ performance analysis is to set the performance index as the H∞ norm of the evaluation function and to obtain the performance of the robust controller by optimizing the H∞ norm in real rational function space.

The H∞ performance reflects the energy ratio of the output signal to the input signal under the action of an energy-bounded signal, which can be used to measure the strength of anti-interference ability of the system. It is defined as the peak value of the maximum singular value of the system frequency response. As shown in (17), the maximum singular value represents the maximum growth rate that can be reached within a certain period of time, and the singular vector corresponding to the maximum singular value is the fastest growing initial perturbation direction. Therefore, the H∞ norm is applicable to the signal gain that simultaneously describes the degree of uncertainty of the object in the control system and the interference of the input end to the error of the output end.

$$\|F\|_\infty = \sup_{\mathrm{Re(s)}>0} \overline{\sigma}\left[F\left(\mathrm{s}\right)\right] = \sup_{\omega\in R} \overline{\sigma}\left[F\left(j\omega\right)\right] \tag{17}$$

F is a matrix function which is parsed and bounded in the right half-plane and $\overline{\sigma}$ represents the maximum value of the singular value. Shown in Figure 3 is standard H∞ control model.

In Figure 3, Y is the observed signal; U means the output of the controller which is a generalized control signal; $G_p$means a generalized controlled object; Z represents the evaluation output. W means the outside interference. In the design, we hope that Z is as small as possible. The problem of H∞ optimal control is to design a stabilization controller such that the H∞ norm of the transfer function G_{wz} from W to Z is minimal. It means that there is a small γ that satisfies the following relationship:

$$\left\|G_{wz}\right\|_\infty = \sup\frac{\|z\|^2}{\|w\|^2} < \gamma \tag{18}$$

Satisfying the above relationship, the system is considered to have a good H∞ performance, multiplicative perturbation, $u = [u]$ is the output of EPS controller, n is the sensor noise, and $y = [i]$ is the output of the controlled system.

Converting the model of Figure 4 to the standard H∞ control model based on hybrid sensitivity shown in Figure 5, it can be seen that it meets the standard H∞ model shown in Figure 3. As is shown in Figure 5, the weighting functions *Ws, Wr, Wt* are introduced; the error *e*, the controller output *u*, and the output y of the controlled system are adjusted by the weighting function, and the target to be controlled is highlighted to obtain better system performance. As can be observed in the comparison between Figures 4 and 5, the sensor noise n and the multiplicative perturbation factor Δ_m in Figure 4 do not appear in Figure 5 because the weighting functions *Ws*, *Wr*, and *Wt* limit these interference factors.

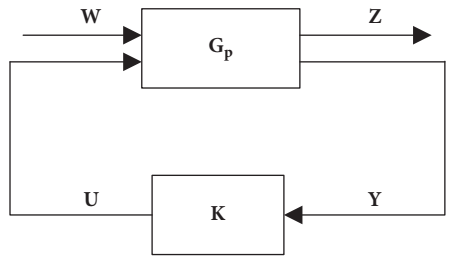

Figure 3: Standard H∞ control model.

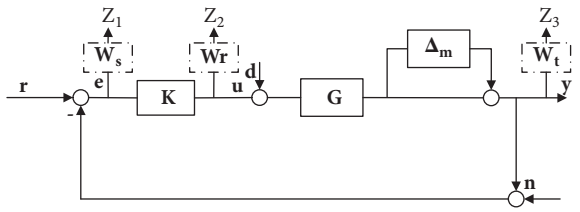

Figure 4: EPS generalized control model with model perturbation and interference.

The multiplicative uncertainty Δ_m of the model exists in the generalized controlled object in the form of W_t, guaranteeing that $\|W_t\|_\infty \geq \|\Delta\|_\infty$.

The transfer function of the system from external interference input W to $Z = [Z_1\ Z_2\ Z_3]^T$ is $G_{zw} = [W_sS\ W_rR\ W_tT]^T$, S, R, T are, respectively, the closed-loop transfer function of the reference input W to the tracking error e, the control output u and the measurement output y, and $R = K * S$ Therefore, the design problem of robust controller is transformed into finding the rational function controller K, and $\|G_{wz}\|_\infty \leq \gamma$. When $\|G_{wz}\|_\infty \leq 1$, this problem belongs to the standard H∞ suboptimal optimization problem.

Research and analysis show that *Ws (s)* should have high-gain and low-pass characteristics; *Wt (s)* represents the requirement for robust stability and should have high-pass filter characteristics; *Wr (s)* is generally taken as a real constant, and considering that the order of the three weighting functions should be as small as possible to reduce the order of the controller, the three weighting functions in this paper are defined as follows:

$$W_s = a_1 \frac{b_1 s + 1}{c_1 s + 1}$$
$$W_r = a_2 \tag{19}$$
$$W_t = a_3 \frac{b_3 s + 1}{c_3 s + 1}$$

4. EPS Generalized Equation of State

Take the state vector:

$$x = [x_1\ \ x_2\ \ x_3\ \ x_4\ \ x_5\ \ x_6]^T = [\alpha\ \ \dot{\alpha}\ \ \delta\ \ \dot{\delta}\ \ \theta\ \ \dot{\theta}]^T \tag{20}$$

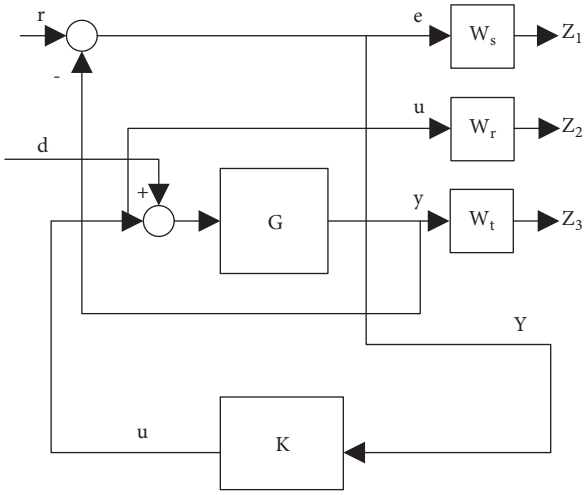

Figure 5: Standard H∞ control model based on hybrid sensitivity.

From (1)-(9), we can get the following:

$$\dot{x}_2 = \ddot{\alpha} = \frac{1}{J_s}\left(\mathrm{T_h} - \mathrm{K}_s\alpha + \mathrm{K_s}\delta - \mathrm{B_s}\dot{\alpha}\right)$$
$$\dot{x}_4 = \ddot{\delta} = \frac{1}{J_c}\left(\mathrm{K_m}\theta - \left(K_m + \mathrm{K_c} + K_s\right)\delta - \mathrm{T_r} - B_c\dot{\delta}\right) \tag{21}$$
$$\dot{x}_6 = \ddot{\theta} = \frac{1}{J_m}\left(\frac{\mathrm{K_t}u}{R+L} - \frac{K_m}{g_1} + \frac{K_m}{g_1}\delta - \left(\frac{\mathrm{K_t K_e}}{R+L} + B_m\right)\dot{\theta}\right)$$

External inputs of the forklift EPS system are mainly the power motor control voltage u, the driver's operating torque Th, and the pavement interference Tr. These signals constitute the EPS generalized control signal:

$$U = [d\ \ u]^T = [T_h\ \ T_r\ \ u]^T \tag{22}$$

The output of generalized controlled system is as follows:

$$Y = [e] \tag{23}$$

The output of system evaluation is

$$\mathrm{Z} = [W_s e\ \ W_r u\ \ W_t \mathrm{y}]^T \tag{24}$$

where, $y = [i]$ is the output of the system, $Z = W_1 * \begin{bmatrix} e \\ u \\ y \end{bmatrix}$, $W_1 = \begin{bmatrix} W_s & 0 & 0 \\ 0 & W_r & 0 \\ 0 & 0 & W_t \end{bmatrix}$, so we can construct a controlled generalized object without a weighting function: $G_p{}' : U \longrightarrow \begin{bmatrix} Z' \\ Y \end{bmatrix}$

$$Z' = [e\ \ u\ \ y]^T \tag{25}$$

where the control power error e is calculated by (13), and the power torque $T\alpha*$ of the ideal power current output is obtained from (3):

$$T_\alpha{}^* = g_1\left(T_m - J_m\ddot{\theta} - B_m\dot{\theta}\right) \tag{26}$$

From (3), (18), and (24), we can get the control system power error e; the expression is as follows:

$$e = \left(K_m - \frac{K_m}{g_1}\right) + \left(\mathrm{K_t kK_s} - \mathrm{K_m} + \frac{K_m}{g_1}\right)\delta - K_t k K_s \alpha - \frac{K_e K_t}{R+L}\dot{\theta} + \frac{K_t}{R+L}u \tag{27}$$

Generalized control object with weighting function is

$$G_p = \begin{vmatrix} W_1 & \\ & I \end{vmatrix} * G_p{}' \tag{28}$$

Combined with the electric forklift data of TFC20 front steering electric forklift, we can get the state space equation of the system as

$$\begin{aligned} \dot{x} &= Ax + BU \\ Z' &= C_1 x + D_1 U \\ Y &= C_2 x + D_2 U \end{aligned} \tag{29}$$

where

$$A = \begin{bmatrix} 0 & 1 & 0 & 0 & 0 & 0 \\ \frac{-K_s}{J_s} & \frac{-B_s}{J_s} & \frac{K_s}{J_s} & 0 & 0 & 0 \\ 0 & 0 & 0 & 1 & 0 & 0 \\ \frac{K_s}{J_c} & 0 & \frac{-(K_s + K_s + K_c)}{J_c} & \frac{-B_s}{J_c} & \frac{K_m}{J_c} & 0 \\ 0 & 0 & 0 & 0 & 0 & 1 \\ 0 & 0 & \frac{K_m}{g_1 * J_m} & 0 & \frac{-K_m}{g_1 * J_m} & \frac{-((K_t * K_e)/(R+L) + B_m)}{J_m} \end{bmatrix}$$

$$B = \begin{bmatrix} 0 & \frac{1}{J_s} & 0 & 0 & 0 & 0 \\ 0 & 0 & 0 & \frac{1}{J_c} & 0 & 0 \\ 0 & 0 & 0 & 0 & 0 & \frac{K_t}{J_m * (\mathrm{R+L})} \end{bmatrix}^{\mathrm{T}}$$

$$C_1 = \begin{bmatrix} -K_t * k * K_s & 0 & K_t * k * K_s + \left(\frac{1-g_1}{g_1}\right)K_m & 0 & 0 & \frac{-K_t K_e}{R+L} \\ 0 & 0 & 0 & 0 & 0 & 0 \\ 0 & 0 & 0 & 0 & 0 & \frac{-K_e}{R} \end{bmatrix},$$

$$D_1 = \begin{bmatrix} 0 & 0 & \frac{K_t}{R+L} \\ 0 & 0 & 1 \\ 0 & 0 & \frac{1}{R} \end{bmatrix},$$

$$C_2 = \begin{bmatrix} -K_t * k * K_s & 0 & K_t * k * K_s + \left(\frac{1-g_1}{g_1}\right)K_m & 0 & 0 & \frac{-K_t K_e}{R+L} \end{bmatrix}$$

$$D_2 = \begin{bmatrix} 0 & 0 & 0 \end{bmatrix} \tag{30}$$

5. Robust Control Based on Genetic Optimization

Genetic algorithms provide a universal solution to the optimization problem of complex systems. They have strong robustness and have been widely used. However, in practical applications, genetic algorithms involve the selection of fitness functions and specific parameters.

5.1. Significance of the Weighting Function. The reasonable setting of the weighting function can effectively restrain the influence of interference and accurately track the input signal. Through the weighting function, the error e, the controller output u, and the controlled system output y are adjusted to get the best control target. where *Ws* is to better reflect the size of the sensitivity function S at low frequency, which reflects the follow-up of the actual power current provided

by the motor to the ideal power current. The selection of Wt mainly reflects the inherent properties of the system, including the uncertainty of system model, sensor noise, and other interference factors; the weighting function of the input u corresponds to the selection of Wr in order to remove the high frequency components of the input and avoid its interference with the system. Therefore, adjusting parameters of weighting function is very important. Genetic algorithm is proposed to optimize the parameters of weighting function in order to obtain better robustness of the system.

5.2. Determination of Constraint Function of Genetic Algorithm. The function optimization problem is to satisfy certain constraints and to make certain performance indexes of the system get the maximum or minimum, so as to satisfy certain optimal metrics of the system. According to robust control requirements of EPS system, the constraint function is constructed as follows.

(1) $\delta_1 = 20 * \lg[\sigma'[G_P(j\omega)]]$. σ' represents the maximum singular value, and the maximum singular value represents the maximum growth rate that the perturbation can achieve within a certain period of time, and δ_1 represents the general indicator of robust design, that is, the influence of uncertain factors on the generalized controlled object, when $\delta_1 < 0$, take $\varphi_1 = \sigma'[G_p(j\omega)]$; when $\delta_1 \geq 0$, take $\varphi_1 = 100$.

(2) $\delta_2 = 20 * \lg[\sigma'[W_s(j\omega) \cdot S(j\omega)]]$. The product of Ws and S represents the transfer function of the external interference W to the evaluation output $Z1$, while Ws is the weight of the error e, and δ_2 reflects the ability of the system to resist interference. When $\delta_2 < 0$, take $\varphi_2 = \sigma'[W_s(j\omega) \cdot S(j\omega)]$; when $\delta_2 \geq 0$, take $\varphi_2 = 10$.

(3) $\delta_3 = 20 * \lg[\sigma'[W_t(j\omega) \cdot T(j\omega)]]$. The product of Wt and T represents the transfer function of the external interference W on the evaluation output $Z3$, and Wt is the weight of the output y of the controlled system, reflecting the inherent stability properties of the system, including factors such as model uncertainty, when $\delta_3 < 0$, take $\varphi_3 = \sigma'[W_T(j\omega) \cdot T(j\omega)]$, and when $\delta_3 \geq 0$, take $\varphi_3 = 10$.

(4) $\delta_4 = 20 * \lg[\sigma'[W_r(j\omega) \cdot R(j\omega)]]$. The product of Wr and R represents the transfer function of the external interference W on the evaluation output $Z2$, and Wr is the weight of the controller output u, δ_4 represents the control of the motor output, in order to remove the high-frequency interference of the motor voltage output, when $\delta_4 < 0$, take $\varphi_4 = \sigma'[W_r(j\omega) \cdot R(j\omega)]$ and when $\delta_4 \geq 0$, take $\varphi_4 = 10$.

δ_3 and δ_4 reflect the requirements of system robustness, that is, whether the system can maintain stability and meet certain performance requirements under the interference of uncertain factors.

(5) $\delta_5 = 20 * \lg[\sigma'[W_s^{-1}(j\omega)] + \sigma'[W_t^{-1}(j\omega)]]$. When $\delta_5 < 0$, take $\varphi_5 = \sigma'[W_s^{-1}(j\omega)] + \sigma'[W_t^{-1}(j\omega)]$, and when $\delta_5 \geq 0$, take $\varphi_5 = 100$.

δ_5 requires that the bands of Ws and Wt do not intersect.

Objective function $f = \sum_{i=1}^{5} \varphi_i$, and fitness function takes the minimum F=f.

5.3. Optimization Results. The coefficients of $a_1, b_1, c_1, a_2, a_3, b_3, c_3$ are coded using binary coding to determine the search domains of the respective coefficients, which are connected in series to form a chromosome or an individual.

Determine the genetic algebra $G_e = 200$, crossover probability $P_c = 0.7$, mutation probability $P_m = 0.08$, and population size $M = 110$.

The selection operator uses a proportional selection factor, depending on the probability of its individual fitness. If the fitness of individual i is f_i, then the probability that the individual is selected is $\Phi_i = f_i / \sum_{k=1}^{M} f_k$.

$a_1 = 198$, $b_1 = 0.0040$, $c_1 = 6.68$, $a_2 = 0.0207$, $a_3 = 0.651$, $b_3 = 0.0078$, $c_3 = 0.0005$ can be got by using MATLAB genetic algorithm optimization box. The corresponding robust controller is

$$\mathrm{K}(s) = \frac{1.6 * 10^5 (s + 513)(s + 103)(s + 9)(s + 2)\left(s^2 + 9s + 580\right)}{(s + 2.16)(s + 601)(s + 246)(s + 89)(s + 0.26)\left(s^2 + 13s + 47\right)} \tag{31}$$

At this point, $\|G_{zw}\|_\infty = 0.8113 < 1$, which meets the robust control objectives.

6. Robust Controller Design

In this paper, we can solve the H∞ controller by using the LMI toolbox in MATLAB.

The model of the controlled system is equivalent to the following formula by (29):

$$\begin{aligned} \dot{x} &= Ax + B_1 w + B_2 u \\ Z &= C_1 x + D_{11} w + D_{12} u \\ Y &= C_2 x + D_{21} w + D_{22} u \\ u &= kY \end{aligned} \tag{32}$$

The controller K required to set up the system is as follows:

$$\begin{aligned} \dot{x}_k &= A_k x_k + B_k Y \\ u &= C_k x + D_k Y \end{aligned} \tag{33}$$

where the controller status is represented as x_k, $K = \begin{bmatrix} A_k & B_k \\ C_k & D_k \end{bmatrix}$ is the controller sought in this paper, and A_k, B_k, C_k, D_k are the parameters to be determined

Applying controller K, i.e., applying (33) to the system represented by (32), results in the following closed loop system:

$$\begin{aligned} \dot{\zeta} &= A_{c1}\zeta + B_{c1} w \\ z &= C_{c1}\zeta + D_{c1} w \end{aligned} \tag{34}$$

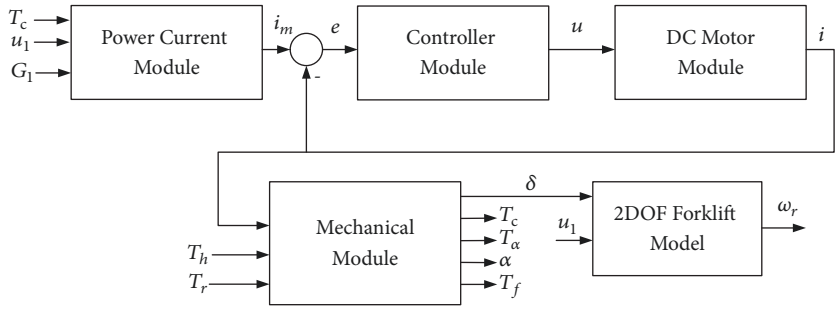

Figure 6: The overall diagram of the EPS system.

where

$$\zeta = \begin{bmatrix} x \\ \dot{x} \end{bmatrix},$$

$$A_{c1} = \begin{bmatrix} A + B_2 D_k C_2 & B_2 C_k \\ B_k C_2 & A_k \end{bmatrix},$$

$$B_{c1} = \begin{bmatrix} B_1 + B_2 D_k D_{21} \\ B_k D_{21} \end{bmatrix}, \quad (35)$$

$$C_{c1} = \begin{bmatrix} C_1 + D_{12} D_k C_2 & D_{12} C_k \end{bmatrix},$$

$$D_{c1} = D_{11} + D_{12} D_k D_{21}.$$

This paper applies the LMI toolbox in MATLAB to solve the H∞ controller K(s). The H∞ solver Hinflmi based on the linear matrix inequality processing method provided by the LMI toolbox is used to solve the output feedback H∞ controller K(s) of the EPS system corresponding to the controlled generalized object transfer function matrix Gp(s). The function form of the Hinflmi solver is as follows:

$$[gopt, K] = \text{hinflmi}\left(G_p, [p \;\; m], h\right) \quad (36)$$

where γ is the performance index of H∞ controller; K represents the H∞ controller; p and m indicate that the input p and output m of the H∞ controller; that is, the system measurement output y is p-dimension, and the system control input u is m-dimensional; in this paper $[p \;\; m] = [1 \;\; 1]$, h indicates that the operation result will get a robust H∞ controller, where h is set to 1, indicating that the obtained controller is a standard H∞ controller, and the performance index γ of the EPS closed-loop system is 0.9137; that is, for the uncertain EPS controlled system in this paper, there is a controller that makes it progressively stable. The system shifts the external input W to the transfer function matrix of the evaluation output Z $\|T_{WZ}\|_\infty = 0.9137 < 1$, indicating that the H∞ controller is a standard H∞ controller, from which it can also be stated that the requested H∞ controller can guarantee the asymptotic stability of the requested system.

7. Simulation Results and Analysis

In order to verify the effect of robust control based on genetic optimization, combined with TFC20 forklift data, PID control is a traditional control method, and robust control is widely used to control vehicles; as the industrial handling vehicles, forklifts have higher requirements for stability, the genetic robust control algorithm is compared under the same conditions.

7.1. Simulation Modeling. In simulation modeling, MATLAB/Simulink components are used. According to the above analysis, the simulation model of EPS for electric forklift consists of a DC motor module, a mechanical steering system module, an ideal power characteristic module, a controller module, and a 2DOF forklift model. Connect the input and output variables of the above parts to get the overall model of the electric forklift EPS system, as shown in Figure 6.

The centroid speed of forklift u_1, rang[0-15], unit: km/h; G, rang[0-1500], unit: kg; T_h is the hand-wheel torque, rang[0-15], unit: Nm. The main parameters of TFC20 forklift in the simulation are shown in Table 1.

7.2. Analysis of Simulation Results. Firstly, steering performance of electric forklifts is studied with different control methods for hand-wheel torque interference. At this time, the fixed forklift has a full-load mass; i.e., G1 is set to 1500 kg. The amplitude value of the steering step torque input signal Th is set to $8Nm$ to simulate the sudden unilateral rotation of the hand-wheel, and in the interval of 4s—4.5s, input an T_r (T_r=10Nm) signal as road interference in order to test the robustness of the system under different vehicle speeds. Simulation waveforms are shown in Figures 7(a)–7(c).

Then perform a sine signal input test, at this time, keep the forklift speed at 10 km/h which is the normal speed of the forklift. The hand-wheel torque input Th is a sinusoidal signal and it is used to simulate the situation where the hand-wheel rotates left and right. The amplitude is set to 10 Nm, the period is 2πs, and the simulation time is 10 s. Simulation waveforms are shown in Figures 8(a)–8(c).

The step response can largely reflect the dynamic characteristics of the system. In the simulation, the PID controller parameters: P=10, I=10, and D=0. From Figures 7(a)–7(c), under the PID control, the step response curve of the actual power current of the motor and the response curve after adding interference both have a large amount of overshoot; under the robust control, the time response curve becomes smooth, and the overshoot of the response curve after adding

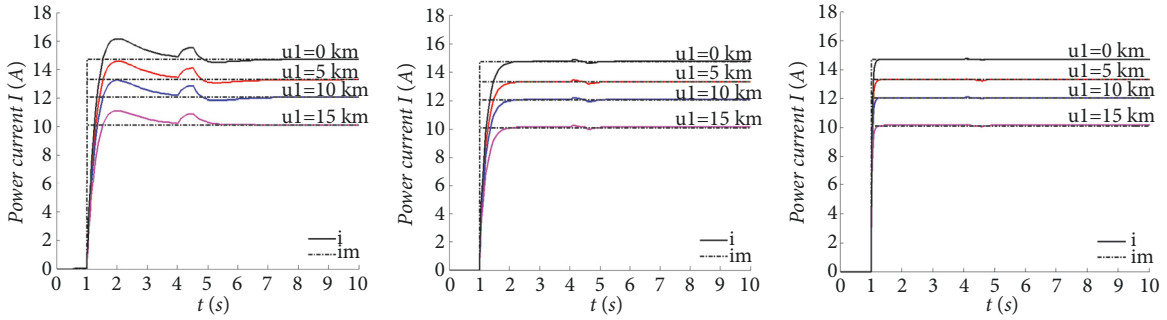

(a) PID control (b) Robust control (c) Genetic optimization robust control

Figure 7: Comparison of step input performance with steering torque interference under different control methods.

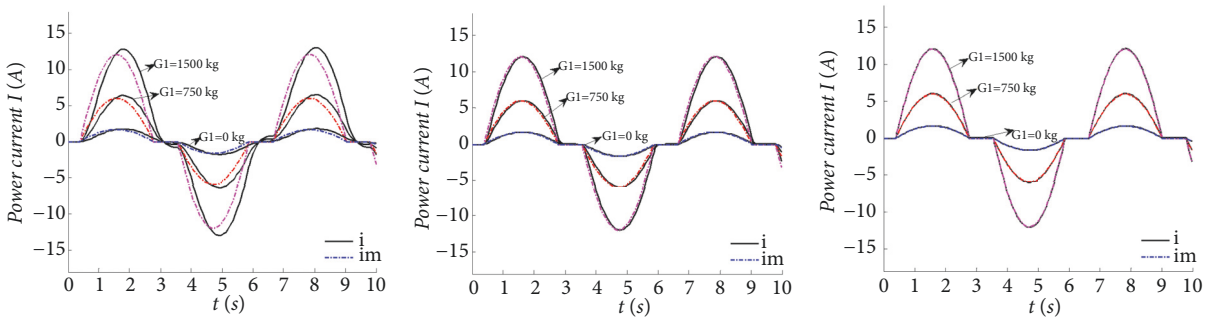

(a) PID control (b) Robust control (c) Genetic optimization robust control

Figure 8: Comparison of sinusoidal input performance under different control methods.

Table 1: Main parameters of forklift.

m (kg)	2340
B_c (kg·m)	0.361
J_c (kg·m)	0.089
J_m (kg·m^2)	$2.250/10^4$
k_1 (N/rad)	-62618
k_2 (N/rad)	-110245
a (m)	1.352
b (m)	1.485
R (Ω)	0.450
g_1	16.500
L (mH)	3.339

interference also decreases significantly; under genetic optimization robust control, the step response of the actual power current is faster and the current follows well. Moreover, when the forklift's on-board mass and the hand-wheel torque input are the same, if the speed is greater, the power current and power torque will be smaller; thereby it will improve the driver's road feeling and stability of operation and increase the safe driving performance of electric forklifts.

From Figures 8(a)–8(c), under PID control, the actual power current of the motor has a large deviation from the ideal current; under the robust control, the actual current and the ideal current follow ability are obviously enhanced, but they are still not fully followed; under the genetic optimization robust control, the actual current is almost consistent with the ideal current.

It can be seen from the above simulation curve that PID control directly takes the error between the target and the actual behavior is not completely reasonable, because the system output has a certain inertia, it is impossible to jump, and the target value is given outside the system, it can be jumped. Use the error between them directly to eliminate the error means that the amount that is impossible to jump is used to track the amount that can be jumped. This way of "directly taking the error between the target and the actual behavior to eliminate the error" often causes the initial control force to be too large and the system behavior to overshoot. The overshoot of the PID under the interference condition is very large, which would be very dangerous if the actual PID parameter is not adjusted well in practice. For the uncertain interference problem faced by the system, the robust control can be well solved. Under the same interference conditions, we can see that under the interference condition, the overshoot of the robust control is small, it means that the current is more stable, and it is mainly due to the robust control system's ability to maintain performance when face the interference. At the same time, we can see that the control effect of genetic optimization robust control is the best; it can be understood that genetic algorithms provide a universal solution to the optimization problem of complex systems, and they have strong robustness, and the function

optimization problem is to satisfy certain constraints and to make certain performance indexes of the system get the maximum or minimum, so as to satisfy certain optimal metrics of the system, we combine genetic algorithms and robust control to achieve a more stable control effect.

In summary, robust control can better provide the electric forklift with suitable power torque, while genetic optimization can provide better parameters of the weighting function, so as to design a better controller for the electric forklift to provide power torque which is closer to the ideal value. Moreover, when the forklift's vehicle speed and the hand-wheel torque input are the same, when the vehicle's mass is greater, the ideal power current will be greater, and the motor will provide a greater power torque which will reduce the driver's burden.

7.3. Comparison of Steering Stability Performance of Electric Forklift under Different Control Methods. As the safety of the driver and the cargo should be considered during the operation of the forklift, the stability of the power steering system of the electric forklift is also a consideration of the EPS system. The yaw rate refers to the rotation of the vehicle about the vertical Z axis, which reflects the stability of the vehicle to some extent. Therefore, the observation target of the steering stability of electric power steering system is represented by the transient response characteristics of the yaw rate [26–28].

Aiming at the forklift's full-load conditions, this paper compares the steering stability of electric forklifts under different control methods. In the experiment, the interference input is a superposition of a sinusoidal signal and is used to simulate a random interference scenario on the road, as shown in Figure 9.

Figure 10 shows the yaw rate response curve under different control methods. It can be seen from Figure 10(a) that, under PID control, the yaw rate response of the electric forklift has significant fluctuations for the input of pavement interference. From Figure 10(b), under the robust control, the yaw rate response curve is significantly smoother, and the yaw rate is slightly reduced. From Figure 10(c), under genetic optimization robust control, the yaw rate response curve is more stable, and the time response speed is faster, and the value of the yaw rate is also slightly decreased. In summary, the robustness and control performance of the optimized robust controller are even better.

8. Conclusion

With the continuous update of automotive electronics technology, various aspects of the EPS system have breakthroughs in different degrees of development. The EPS system was developed from the initial application for small cars to the application for large cars and handling vehicles and its applications have become more and more widespread and EPS systems can improve the vehicle's handling stability at high speed. Compared with the traditional steering systems such as the mechanical steering system and the hydraulic steering system, the electric power steering system has the characteristics of high control flexibility, a simple structure, and high safety. Therefore, researches on the electric power steering systems for electric forklifts have important engineering significant applications [29–31].

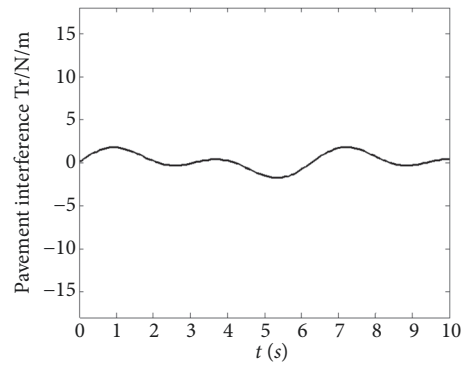

Figure 9: Diagram of the pavement interference.

The research object of this paper is the electric power steering system of the TFC20 front-wheel steering electric forklift. The EPS dynamics model of the electric forklift is first established and the control target is given. Then the control model is established and the generalized state equation of the EPS is derived. Finally, the robust H∞ control scheme is based on genetic algorithm.

Simulations verify that the robust H∞ controller based on the closed-loop current control strategy can better cope with the system uncertainty perturbation caused by sudden pavement interference, and the controller makes the forklifts have better power steering characteristic and stability. The simulation results also show that the robustness of the robust H∞ controller optimized by the genetic algorithm is better, and the stability of the forklift is also better.

Nomenclature

J_s: Moment of inertia about the hand-wheel
J_c: Moment of inertia about output shaft
J_m: Moment of inertia about the motor
B_s: Damping coefficient of the hand-wheel
B_c: Damping coefficient of the output shaft
B_m: Damping coefficient of the motor
T_c: Output torque of the torque sensor
T_h: Operating torque of the driver
T_f: Equivalent steering resistance torque to output shaft
T_α: Power torque of motor output
T_m: Electromagnetic torque of the motor
g_1: Gear ratio from output shaft to motor
g_2: Gear ratio from output shaft to the front wheel

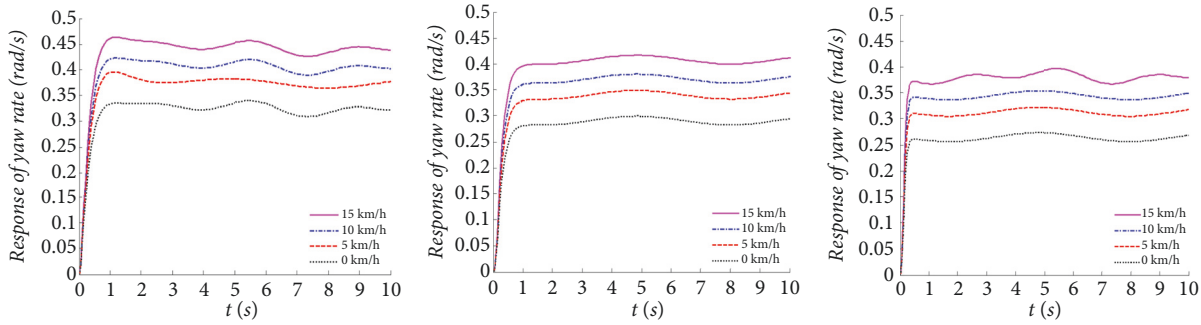

(a) PID control (b) Robust control (c) Genetic optimization robust control

Figure 10: Comparison of yaw rate response curve under different control methods.

K_s:	Stiffness of the torque sensor
K_e:	Back EMF coefficient of motor
K_t:	Electromagnetic torque coefficient of motor
K_p:	Ratio coefficient between wheel resistance torque and front wheel
K_c:	Equivalent lateral stiffness to the output shaft
K_m:	Rigidity coefficient of motor
α:	Equivalent corner to the output shaft from hand-wheel
δ:	Equivalent corner to the output shaft from steering wheel
θ:	Rotation angle of steering motor
u:	Terminal voltage of motor
i:	Actual power current of the motor
i_m:	Ideal power current of the motor
R:	Equivalent resistance of motor
T_r:	Pavement interference
u_1:	Vehicle speed
K:	Slope of the power current
G_1:	Quality of the vehicle
$f_s(\alpha, \dot{\alpha})$, $f_c(\delta, \dot{\delta})$, $f_m(\theta, \dot{\theta})$:	Nonlinear part of the system and time-varying and other factors.

Data Availability

The data used to support the findings of this study are included within the article.

Conflicts of Interest

The authors declare that they have no conflicts of interest.

Acknowledgments

This work is supported by National Natural Science Foundation (NNSF) of China under Grant 51577046, the National Key Research and Development Plan "Important Scientific Instruments and Equipment Development" Grant no. 2016YFF0102200.

References

[1] L. Fan, B. Zhou, and H. Zheng, "A New Control Strategy for Electric Power Steering on Low Friction Roads," *SAE International Journal of Passenger Cars—Mechanical Systems*, vol. 7, no. 3, pp. 972–980, 2014.

[2] Y.-C. Hung, F.-J. Lin, J.-C. Hwang, J.-K. Chang, and K.-C. Ruan, "Wavelet fuzzy neural network with asymmetric membership function controller for electric power steering system via improved differential evolution," *IEEE Transactions on Power Electronics*, vol. 30, no. 4, pp. 2350–2362, 2015.

[3] W. Kim, Y. S. Son, and C. C. Chung, "Torque-Overlay-Based Robust Steering Wheel Angle Control of Electrical Power Steering for a Lane-Keeping System of Automated Vehicles," *IEEE Transactions on Vehicular Technology*, vol. 65, no. 6, pp. 4379–4392, 2016.

[4] D. Lee, K.-S. Kim, and S. Kim, "Controller Design of an Electric Power Steering System," *IEEE Transactions on Control Systems Technology*, vol. 26, no. 2, pp. 748–755, 2018.

[5] J.-Q. Gong, W. Yang, and W.-W. Heng, "Heavy truck EPS system simulation based on PSO optimization fuzzy control," in *Proceedings of the International Conference on Intelligent Transportation, Big Data and Smart City, ICITBS 2015*, pp. 446–449, December 2015.

[6] D. Saifia, M. Chadli, H. R. Karimi, and S. Labiod, "Fuzzy control for Electric Power Steering SYStem with assist motor current input constraints," *Journal of The Franklin Institute*, vol. 352, no. 2, pp. 562–576, 2015.

[7] S. Lu, M. Lian, M. Liu, C. Cho, and C. Piao, "Adaptive fuzzy sliding mode control for electric power steering system," *Journal of Mechanical Science and Technology*, vol. 31, no. 6, pp. 2643–2650, 2017.

[8] I. Mousavinejad and R. Kazemi, "Variable structure controller design for steer-by-wire system of a passenger car," *Journal of Mechanical Science and Technology*, vol. 28, no. 8, pp. 3285–3299, 2014.

[9] C. Chitu, J. Lackner, M. Horn, P. S. Pullagura, H. Waser, and M. Kohlböck, "Controller design for an electric power steering system based on LQR techniques," *COMPEL - The International Journal for Computation and Mathematics in Electrical and Electronic Engineering*, vol. 32, no. 3, pp. 763–775, 2013.

[10] L. Gao, L. Jin, F. Wang, Y. Zheng, and K. Li, "Genetic algorithm-based varying parameter linear quadratic regulator control for four-wheel independent steering vehicle," *Advances in Mechanical Engineering*, vol. 7, no. 11, pp. 1–14, 2015.

[11] N. Mehrabi, J. McPhee, and N. L. Azad, "Design and evaluation of an observer-based disturbance rejection controller for electric power steering systems," *Proceedings of the Institution of Mechanical Engineers, Part D: Journal of Automobile Engineering*, vol. 230, no. 7, pp. 867–884, 2016.

[12] M. T. Do, Z. Man, C. Zhang, H. Wang, and F. S. Tay, "Robust sliding mode-based learning control for steer-by-wire systems in modern vehicles," *IEEE Transactions on Vehicular Technology*, vol. 63, no. 2, pp. 580–590, 2014.

[13] F.-J. Lin, Y.-C. Hung, and K.-C. Ruan, "An intelligent second-order sliding-mode control for an electric power steering system using a wavelet fuzzy neural network," *IEEE Transactions on Fuzzy Systems*, vol. 22, no. 6, pp. 1598–1611, 2014.

[14] M. Li and Y. Jia, "Decoupling and robust control of velocity-varying four-wheel steering vehicles with uncertainties via solving attenuating diagonal decoupling problem," *Journal of The Franklin Institute*, vol. 354, no. 1, pp. 105–122, 2017.

[15] C. Dannöhl, S. Müller, and H. Ulbrich, "H ∞-control of a rack-assisted electric power steering system," *Vehicle System Dynamics*, vol. 50, no. 4, pp. 527–544, 2012.

[16] R. Wang, H. Jing, C. Hu, M. Chadli, and F. Yan, "Robust H∞ output-feedback yaw control for in-wheel motor driven electric vehicles with differential steering," *Neurocomputing*, vol. 173, pp. 676–684, 2016.

[17] F. Fachrudin, "Optimization of automatic steering control on vehicle with steer by wire system using particle swarm optimization," *Turkish Journal of Electrical Engineering & Computer Sciences*, vol. 24, no. 1, pp. 541–557, 2016.

[18] R. Abu Hanifah, S. F. Toha, M. K. Hassan, and S. Ahmad, "Power reduction optimization with swarm based technique in electric power assist steering system," *Energy*, vol. 102, pp. 444–452, 2016.

[19] F. Wilhelm, T. Tamura, R. Fuchs, and P. Mullhaupt, "Friction compensation control for power steering," *IEEE Transactions on Control Systems Technology*, vol. 24, no. 4, pp. 1354–1367, 2016.

[20] A. Balachandran and J. C. Gerdes, "Designing Steering Feel for Steer-by-Wire Vehicles Using Objective Measures," *IEEE/ASME Transactions on Mechatronics*, vol. 20, no. 1, pp. 373–383, 2015.

[21] K. Baša and A. Žemva, "Simulation and verification of a dynamic model of the electric forklift truck," *Intelligent Automation and Soft Computing*, vol. 17, no. 1, pp. 13–30, 2011.

[22] Y. Liu and B. Xiao, "Research on modeling and active steering control algorithm for electric forklift steer-by-wire system," *International Journal of Intelligent Systems and Applications*, vol. 8, no. 11, pp. 70–79, 2016.

[23] Y. He and B. Xiao, "Research of the forklift power-assisted steering system based on safety steering speed control," *International Journal On Smart Sensing and Intelligent Systems*, vol. 8, no. 1, pp. 749–765, 2015.

[24] B. Y. Park and J. Shin, "Improved Approach to Robust Control for Type-2 T-S Fuzzy Systems," *Mathematical Problems in Engineering*, vol. 2018, Article ID 9378230, 9 pages, 2018.

[25] S. Di Cairano, H. E. Tseng, D. Bernardini, and A. Bemporad, "Vehicle yaw stability control by coordinated active front steering and differential braking in the tire sideslip angles domain," *IEEE Transactions on Control Systems Technology*, vol. 21, no. 4, pp. 1236–1248, 2013.

[26] S. Yim, "Fault-tolerant yaw moment control with steer - and brake-by-wire devices," *International Journal of Automotive Technology*, vol. 15, no. 3, pp. 463–468, 2014.

[27] G. Xiang and B. Xiao, "Research on variable transmission ratio and yaw rate control strategy of electric forklift steering-by-wire system," *International Journal of Intelligent Systems and Applications*, vol. 8, no. 10, pp. 21–30, 2016.

[28] A. Marouf, M. Djemai, C. Sentouh, and P. Pudlo, "A new control strategy of an electric-power-assisted steering system," *IEEE Transactions on Vehicular Technology*, vol. 61, no. 8, pp. 3574–3589, 2012.

[29] M. B. Baharom, K. Hussain, and A. J. Day, "Design of full electric power steering with enhanced performance over that of hydraulic power-assisted steering," *Proceedings of the Institution of Mechanical Engineers, Part D: Journal of Automobile Engineering*, vol. 227, no. 3, pp. 390–399, 2013.

[30] Z. Xiao and B. Xiao, "Research on all-wheel steering control strategy for the three-wheel forklift," *Journal of Mechanical Science and Technology*, vol. 30, no. 10, pp. 4717–4724, 2016.

[31] Z. Jiang and B. Xiao, "LQR optimal control research for four-wheel steering forklift based-on state feedback," *Journal of Mechanical Science and Technology*, vol. 32, no. 6, pp. 2789–2801, 2018.